JOC The Journal of Organic Chemistry

Article

pubs.acs.org/joc

Rotationally Hindered Biphenyls and Terphenyls: Synthesis, Molecular Dynamics, and Configurational Assignment

Atul Goel,*[,†] Vijay Kumar,[†] Yasmin Hemberger,[‡] Fateh V. Singh,[†] Pankaj Nag,[†] Michael Knauer,[‡] Ruchir Kant,[§] Resmi Raghunandan,[§] Prakas Ranjan Maulik,[§] and Gerhard Bringmann*[,‡]

[†]Medicinal and Process Chemistry Division, CSIR-Central Drug Research Institute, Lucknow, Uttar Pradesh 226031, India

[‡]Institute of Organic Chemistry, University of Würzburg, Am Hubland, D-97074 Würzburg, Germany

[§]Molecular and Structural Biology Division, CSIR-Central Drug Research Institute, Lucknow, Uttar Pradesh 226031, India

Supporting Information

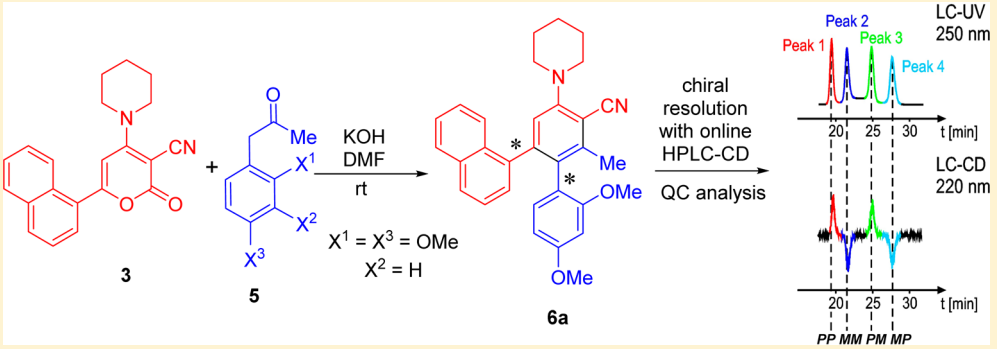

ABSTRACT: Sterically hindered naphthalene-substituted biphenyls and terphenyls were synthesized in good yields, by Michael addition of a conjugate base of core-substituted phenylacetones to substituted 2-oxo-2*H*-pyran-3-carbonitriles at room temperature under alkaline conditions. These diversely functionalized benzenes (1,2-teraryls or 1,3-teraryls), bearing naphthyl and substituted aryl rings, show the phenomenon of atropisomerism, with one or two stereogenic biaryl axes. The resolution of the respective four atropisomers of the naphthalene-substituted biphenyls and terphenyls bearing 1,2-type or 1,3-type chiral biaryl axes was achieved by HPLC on a chiral phase. The absolute stereostructures of **6a** and **9a** were determined by the combination of experimental electronic circular dichroism (ECD) investigations and quantum-chemical circular dichroism (QC-CD) calculations. For the atropisomerization of (1*M*,6*M*)-**6a** and (1*M*,5*M*)-**9a** to their (*M*,*P*)- and (*P*,*M*)-diastereomer, respectively, the possible transition states were investigated and the interconversion barriers ($\Delta G^{\ddagger}$) were theoretically predicted. This study provides a general protocol for the synthesis, resolution, and stereochemical characterization of rotationally hindered naphthalene-substituted biphenyls and terphenyls. The strategy may be applied to investigate other, similarly hindered biaryl or teraryl systems either derived from natural sources or prepared through synthetic approaches.

INTRODUCTION

The study of intrinsic stereodynamic properties of mono-, di-, or multifold axially chiral aromatic compounds is an interesting field of research in chemical sciences, which ultimately leads to develop new chiral catalysts[1] and nanomachines[2] such as molecular rotors, gears, or switches. The motivation for this research results from the fact that nature produces diverse arrays of axially chiral scaffolds such as naphthalene-based biaryls, teraryls, and even highly complicated quarteraryls possessing chemically challenging and biologically impressive properties.[3,4]

Several axially chiral binaphthalene derivatives have been employed for the use as efficient chiral ligands for various enantioselective syntheses. As an example, 2,2′-bis-(diphenylphosphino)-1,1′-binaphthalene (BINAP) has been used as a reliable ligand for various transition-metal-catalyzed reactions.[1] Owing to their inherent chirality, naphthalene-based bi- and oligoaryls have triggered great interest to develop new synthetic strategies aiming at the synthesis of novel aromatic scaffolds with the desired degree of conformational flexibility.[5,6] From a pharmacological point of view, nature creates a broad collection of structurally diverse axially chiral compounds[7−11] and their bioactivities often depend on their axial configurations.[12] Some examples of dimeric natural products having two or even three stereogenic axes, are the dimeric naphthylisoquinoline alkaloids michellamines A and B,[13] mbandakamines A and B,[14] shuangancistrotectorines A−E,[15] and jozimine A_2.[16] Jozimine A_2 showed excellent antiplasmodial activity against the strain NF54 of *Plasmodium falciparum*, with an IC_{50} value of 1.4 nM.[16] Due to the large complexity involved in these naphthalene-based hindered scaffolds, an efficient

Received: July 27, 2016
Published: October 12, 2016

DOI: 10.1021/acs.joc.6b01804
J. Org. Chem. 2016, 81, 10721−10732

Table 1. Synthetic Pathway to the Naphthyl-Substituted Functionalized Biphenyls 6a–f

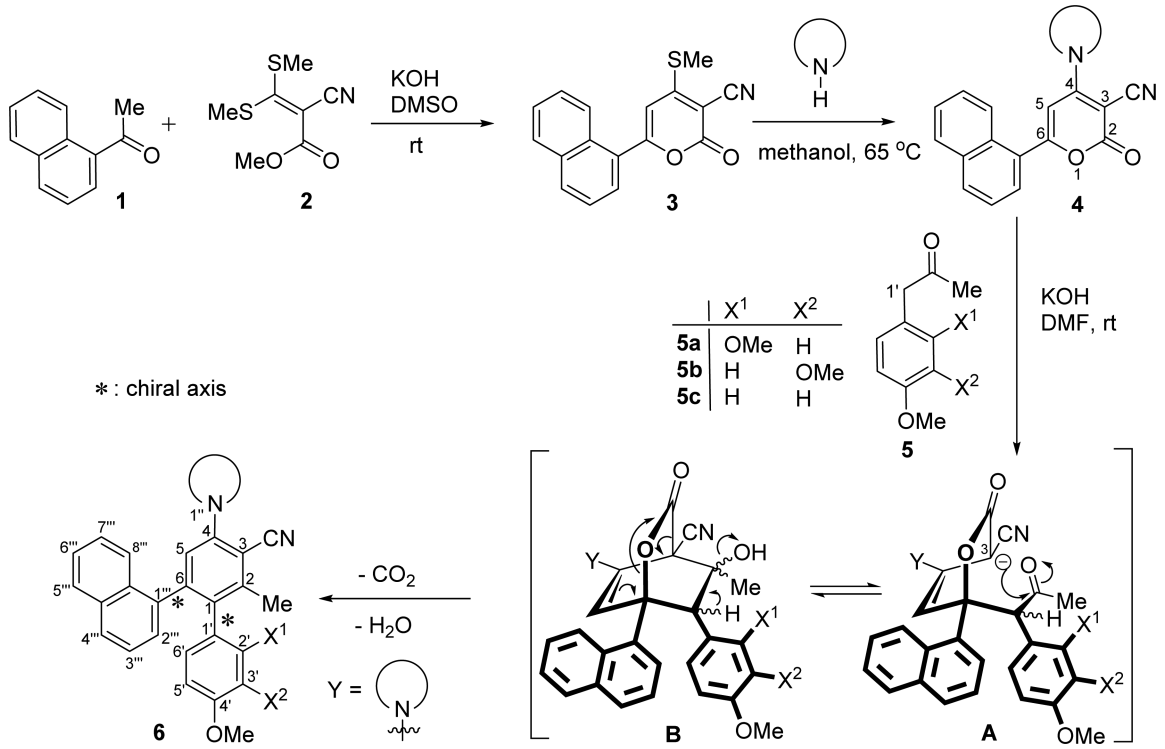

entry	X^1	X^2	Y	time, h	yield, %
6a	OMe	H	*N*-piperidinyl	7	75
6b	H	OMe	*N*-piperidinyl	6	80
6c	H	H	*N*-piperidinyl	6	90
6d	OMe	H	4-methyl-*N*-piperidinyl	9	78
6e	H	OMe	4-methyl-*N*-piperidinyl	6	85
6f	H	H	4-methyl-*N*-piperidinyl	6	92

synthetic route, which furnished template molecules, has already been realized.[17]

The palladium-catalyzed aryl–aryl cross-coupling between electrophilic aromatic halides and organometallic species is a versatile synthetic method for the preparation of diverse arylated benzenes.[18] For the synthesis of axially chiral naphthalene systems, however, significant limitations are known.[4] Actually, the iterative aryl–aryl coupling using tri- or tetrahalides to prepare functionally congested tri- or tetraaryl benzenes via selective aryl transfer is hampered by constraints of the choice of reagents or catalysts and furnishes either low yields of the desired compounds or it is associated with the formation of undesired byproducts.[19]

Recently, we have reported a convenient and general synthetic route for preparing benzenes with di-, tri-, or tetraaryl moieties in a controlled fashion and in a transition-metal-free environment, through simple tailoring of α-oxo-ketene-*S*,*S*-acetals with C–H-activated methylene compounds.[20] We have also demonstrated the synthesis of four-bladed aryl propeller systems having one stereogenic biaryl axis, and their specific peripheral aryl ring interactions around the benzene core.[21] Moving toward sterically more challenging naphthalene systems, we then focused our attention on the preparation and characterization of new axially chiral naphthalene-substituted biphenyls and terphenyls having two 1,2- or 1,3-type stereogenic axes. Sterically congested 1,2-dinaphthylphenyl derivatives with two stereogenic axes have been prepared and resolved by means of cryogenic chromatography on chiral HPLC columns.[22] Recently, 2,3-bis(1-naphthyl)-1,4-diphenyltriphenylene derivatives were prepared by [4 + 2] cycloaddition reactions and were successfully separated into enantiomerically pure compounds by preparative supercritical fluid chromatography on chiral supports.[23] Other axially chiral systems with two chiral axes such as 1,8-diaryl-naphthalene systems have been synthesized by coupling reactions and their stereodynamic properties were examined by NMR and HPLC techniques.[24] In addition, rotationally hindered 1,2- and 1,3-diheteroarylbenzene derivatives were described, and the absolute configurations of their enantiomers were determined using a chemical correlation method in combination with chromatography on a chiral phase.[25]

The determination of the absolute configuration of axially chiral molecules is a crucial, some times challenging task in many areas of research ranging from asymmetric catalysis and biomolecular chemistry to the pharmaceutical industry. One very useful and nowadays commonly used technique for this purpose is circular dichroism (CD) spectroscopy especially in combination with quantum-chemical calculations.[26] The electronic circular dichroism (ECD) probes chirality through molecular electronic transitions appearing in the ultraviolet–visible spectral range, while vibrational circular dichroism (VCD)[27] measures the difference in the absorbance of left- and right-circularly polarized infrared radiation for a vibrational transition and has lately been gaining more importance due to

DOI: 10.1021/acs.joc.6b01804
J. Org. Chem. 2016, 81, 10721–10732

the advantages associated with vibrational spectroscopy.[28] An unprecedented complementarity of the ECD and VCD techniques was demonstrated by Nicu et al.[29] by showing that each method can reveal the structure of a different segment in the investigated chiral biomolecule. However, when a chiral compound has several conformers and has the ability to form strong intermolecular interactions, interpretation of its VCD spectrum is far from straightforward. Therefore, depending upon the complexity of the chiral molecules, both ECD and/or VCD may be employed as a prime tool for investigating the stereochemical behavior of axially chiral molecules.

Herein, we describe a new, simple, and robust pathway for the synthesis of naphthalene-substituted bi- and terphenyl compounds possessing two different types (1,2- or 1,3-type) of stereogenic axes. For compound **6a**, a representative of the naphthalene-substituted biphenyls, and for the naphthalene-substituted terphenyl **9a**, the enantiomeric resolution was exemplarily performed by high-performance liquid chromatography (HPLC) on a chiral phase. HPLC-ECD experiments in combination with quantum-chemical calculations[26] permitted assignment of the absolute configurations of the atropisomers of **6a** and **9a**.

RESULTS AND DISCUSSION

During the course of our studies on the chemical reactivity of 2*H*-pyran-2-ones toward several nucleophilic species, we found that 2-oxo-2*H*-pyran-3-carbonitriles or carboxylic esters are susceptible to Michael addition of a conjugate base of methylene carbonyl compounds (flexible or rigid) at position C6 of the lactone, leading to the formation of a benzene ring at room temperature.[30] This efficient novel pathway to a benzene ring system under mild basic conditions encouraged us to explore the methodology for preparing donor−acceptor based fluorescent dyes for light emitting diodes.[31] The synthetic protocol was further used for the synthesis of naphthalene-substituted hindered biaryl systems as depicted in Table 1.

To synthesize the above-mentioned biphenyls possessing two chiral biaryl axes, *α*-oxo-ketene-*S*,*S*-acetal **2** was treated with 1-(naphthalen-1-yl)ethanone (**1**) following Tominaga's protocol,[32] which furnished the naphthyl-2-pyranone **3** in high yield. In order to incorporate the donor functionalities and to avoid the formation of undesired side products, the methylthiol residue as a leaving group at the C4 position of the lactone **3** was replaced by various secondary amines. This substitution was achieved by heating a mixture of **3** at reflux with piperidine or 4-methylpiperidine in methanol to give the 6-naphthyl-2-oxo-4-amin-1-yl-2*H*-pyran-3-carbonitriles **4a** and **4b** in good yields (Table 1).

Of the three electrophilic centers present in **4**, the one at C6 is highly susceptible to nucleophiles due to the conjugation with even two electron-withdrawing substituents, at C2 and C3 of the pyranone ring. Our approach to prepare the rotationally hindered biphenyls **6a−f** is based on the ring transformation of **4** using the commercially available substituted phenylacetones **5a−c** as a nucleophilic partner (Table 1). The reaction is probably initiated by the Michael addition of the conjugate base of substituted phenyl acetones to form the interconverting intermediates **A** and **B**, followed by elimination of carbon dioxide and water to furnish the naphthalene-substituted biphenyl derivatives **6a−f** in good to excellent yields. For a brief methodology, stirring of an equimolar mixture of 6-(naphthalen-1-yl)-2-oxo-4-(piperidin-1-yl)-2*H*-pyran-3-carbonitrile (**4a**) and 2,4-dimethoxy-phenylacetone (**5a**) at room temperature in the presence of powdered potassium hydroxide (KOH) in dry dimethyl-formamide (DMF) afforded 2′, 4′-dimethoxy-2-methyl-4-(piperidin-1″-yl)-6-(naphthalen-1‴-yl)-biphenyl-3-carbonitrile (**6a**) in 75% yield. The ^{1}H NMR spectrum of **6a** showed a mixture of atropo-diastereomers in the ratio of 51:49 as calculated from the peaks of the methyl and methoxy substituents.

To investigate the 1,2-type 2-fold axial chirality of this new class of biphenyls **6a−f**, a method for the resolution of the respective stereoisomers was exemplarily developed for the four possible atropisomers of 2′,4′-dimethoxy-2-methyl-4-(piperidin-1″-yl)-6-(naphthalen-1‴-yl)biphenyl-3-carbonitrile (**6a**). Unfortunately, several attempts with different achiral and chiral stationary phases failed, even at low temperature. The resolution was finally achieved by the serial connection of two identical Chiracel OD-RH columns (150 × 4.6 mm) under reversed-phase chromatographic conditions (ambient temperature, H_2O/MeCN (15:85) with 0.05% TFA, flow rate = 0.5 mL min^{-1}), leading to four baseline-separated peaks (Peaks 1−4) for the (1*P*,6*M*)-, (1*M*,6*P*)-, (1*P*,6*P*)-, and (1*M*,6*M*)-stereoisomers of **6a** (Figure 1).

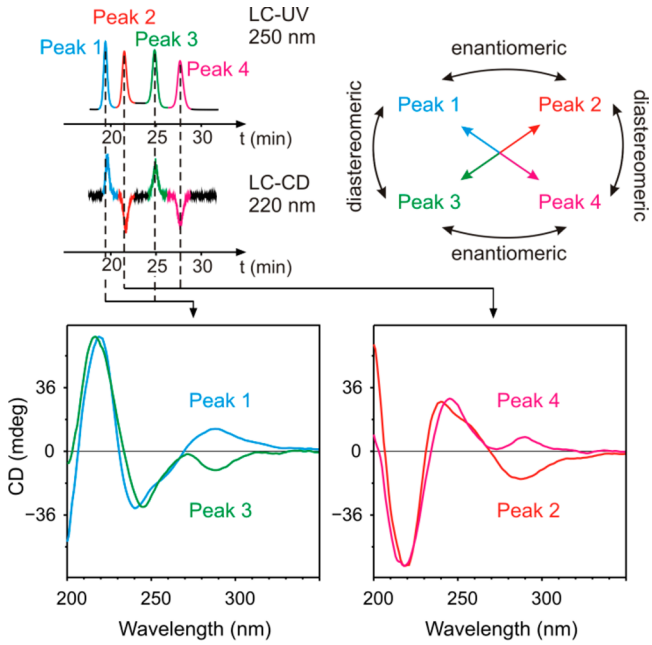

Figure 1. LC-UV and LC-CD traces of the baseline separated peaks and the respective ECD spectra recorded online for the four atropisomers of **6a**.

Since an empirical assignment of the absolute configurations of the four stereoisomers was precluded due to the lack of any precedents and because the circular dichroism (CD) spectra of the two diastereomeric pairs (Peak 1 versus Peak 3, and Peak 2 versus Peak 4) only differed in the very first CD effect at 290 nm, quantum-chemical calculations were performed. Two separate conformational analyses needed to be carried out for the (1*P*,6*M*) isomer and its (1*M*,6*M*) diastereomer concentrating on the dihedral angles depicted in Table 2 (further details are described in Supporting Information). As expected, the conformational arrays at the axes are not independent from each other: If the dihedral angle at the C1,C1′-axis gets larger, the one at the C6,C1‴-axis has to change consecutively to avoid

DOI: 10.1021/acs.joc.6b01804
J. Org. Chem. 2016, 81, 10721−10732

Table 2. Characteristic Dihedral Angles for All the Flexible Parts of 6a, Arbitrarily Depicted for the Minimum Structure of (1*P*,6*M*)-6a

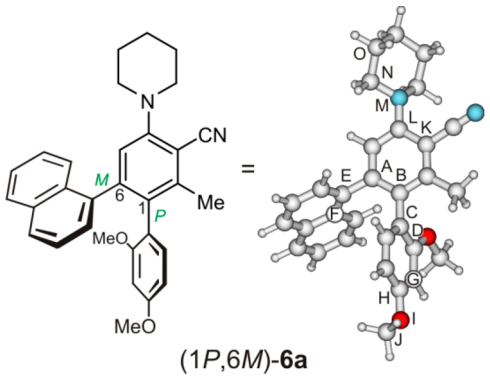

(1*P*,6*M*)-**6a**

θ_{ABCD}		θ_{BAEF}	θ_{GHIJ}	θ_{KLMN}	θ_{LMNO}
(1*P*) 71	(1*M*) −106	−116	180	−66	92
(1*P*) 111	(1*M*) −62	−75	−1	−158	162
				61	
				160	

the otherwise increasing steric and electronic repulsion (Table 2).

Optimization of the 64 possible conformers for each configuration by density functional theory (DFT) with hybrid density function (B3LYP/6-31G*) yielded 16 relevant structures for the (1*P*,6*M*)-configured diastereomer and eight for the (1*M*,6*M*) isomer, in the following abbreviated as (1*P*)-**6a** and (1*M*)-**6a**, respectively. All DFT-optimized minimum structures were subjected to RI-SCS-MP2/def2-TZVP[33,34] (RI: resolution of identity; SCS: spin-component scaled; MP2: Second order Møller−Plesset perturbation theory; TZVP: triple-ζ valence polarized basis set) single-point calculations in combination with conductor-like screening model (COSMO)[35] (H_2O/MeCN: 15/85) to take solvent effects into account. For the energetically relevant conformers—11 in the case of 1*P*-**6a** and 7 for the 1*M*-configured isomer—time-dependent density functional theory (TDDFT) calculations were carried out using the double-hybrid functional TDAB2-PLYP/TZVP[36,37] with COSMO. After Boltzmann weighting and the application of a ultraviolet (UV) correction factor[38] of 7 nm (Figure S21 in Supporting Information), the obtained overall computed CD spectra were compared with the experimental curves and the enantiomeric similarity index (Δ_{ESI})[39] based on the single similarity factors Σ_{fg} for the single enantiomers was calculated (Figure 2). The ESI value reflects the discriminating power between an enantiomeric pair and is therefore a measure for the actual reliability of the assignment of the absolute configuration by the applied quantum-chemical method. The comparison revealed a very good agreement between the CD behavior simulated for the *like*-enantiomers (1*P*,6*P*)- and (1*M*,6*M*)-**6a** with the experimental curves of the more rapidly eluting Peaks 1 (Δ_{ESI} = 78%, $\Sigma_{fg(1P,6P)}$ = 81%) and 2 (Δ_{ESI} = 80%, $\Sigma_{fg(1M,6M)}$ = 84%), whereas the CD spectra calculated for the *unlike*-isomers (1*M*,6*P*)- and (1*P*,6*M*)-**6a** matched very well the ones measured for the more slowly eluting Peaks 3 (Δ_{ESI} = 94%, $\Sigma_{fg(4M,5P)}$ = 94%) and 4 (Δ_{ESI} = 95%, $\Sigma_{fg(1P,6M)}$ = 95%). This permitted unambiguous assignment of the absolute configuration of all four possible stereoisomers (Figure 2).

To confirm the reliability of the excitations obtained by TDAB2PLYP/TZVP (COSMO), especially in regard to the first CD effect at 290 nm, which was crucial for the

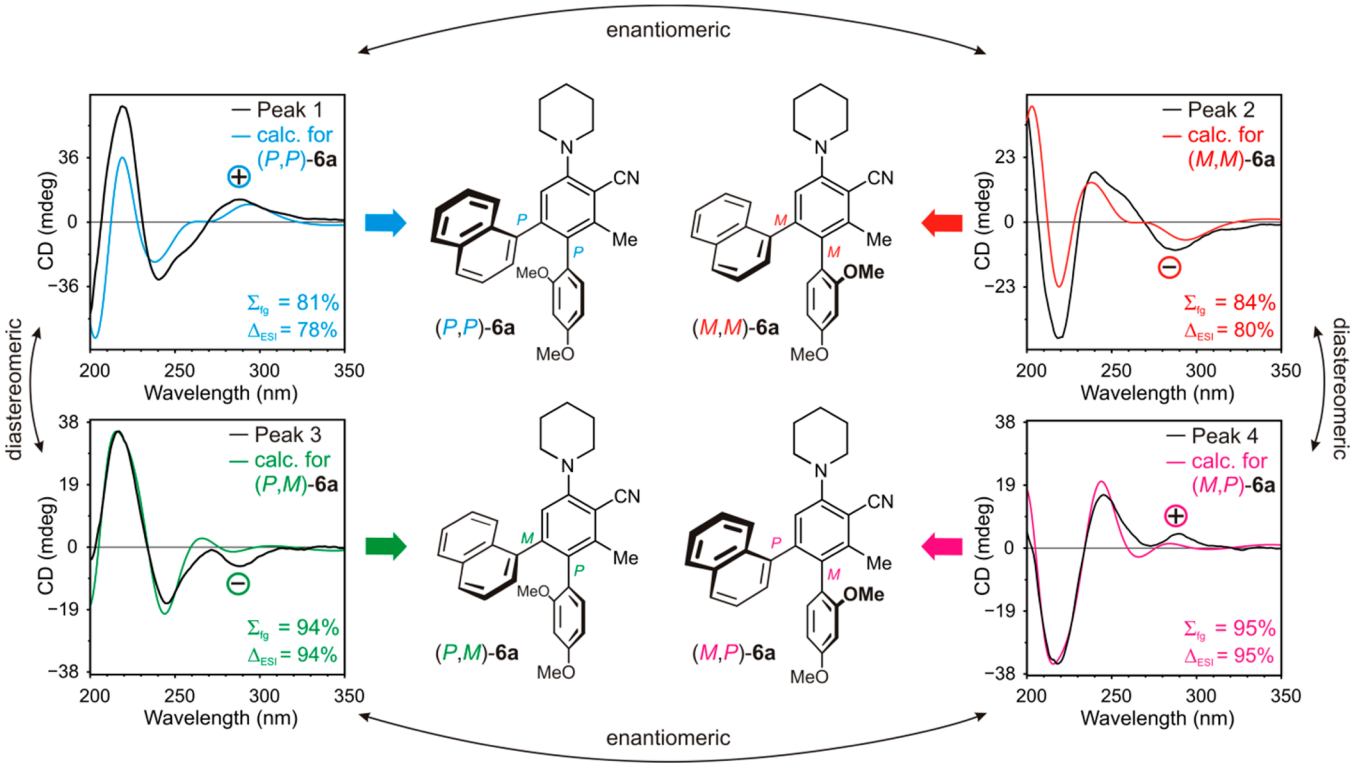

Figure 2. Assignment of the absolute configuration of all four diastereomers—(1*P*,6*P*)-, (1*M*,6*M*), (1*P*,6*M*)-, and (1*M*,6*P*)-**6a**—by comparison of the experimental CD curves with the spectra−quantum-chemically calculated, using B2PLYP/TZVP with COSMO.

DOI: 10.1021/acs.joc.6b01804
J. Org. Chem. 2016, 81, 10721−10732

differentiation between the diastereomeric pairs of Peak 1 versus Peak 3, and of Peak 2 versus Peak 4, more accurate ab initio RICC2/def2-SVP[40] (RI: resolution of identity; CC2: approximated coupled cluster singles and doubles; SVP: split-valence polarized basis set) calculations were used as a reference. However, these coupled-cluster calculations are very time-consuming and, thus, were only carried out for the first ten transitions of the global minimum of each of the diastereomers (1*P*,6*M*)- and (1*M*,6*M*)-**6a**, which already covered the wavelength region of 330 to 240 nm, implying the existence of some so-called ghost states[41] in the TD calculations (17 states). Nevertheless, the comparison of the CD spectra calculated with RICC2 and TDDFT showed a very good agreement, especially for the first CD effect, which is so important for the determination of the absolute configuration of the atropo-diastereomers, thus, corroborating the TDAB2-PLYP/TZVP (COSMO) results (Figure 3).

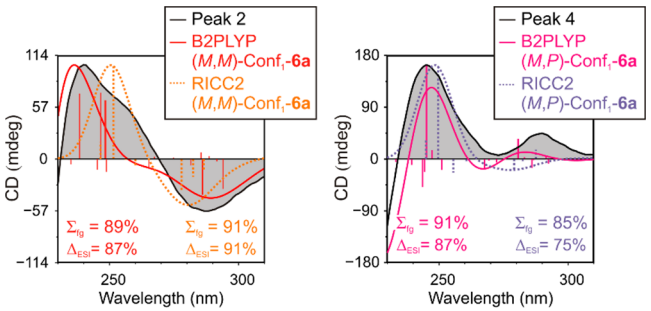

Figure 3. Single excited states and the corresponding CD curves calculated for the global minima of (1*M*,6*M*)-**6a** (left) and (1*M*,6*P*)-**6a** (right) with B2PLYP (shift: 7 nm) and RICC2 (shift: 30 nm).

To investigate the dynamics of an interconversion process of the atropo-diastereomers of **6a**, the transition states TS_{Aryl} and $TS_{Naphthyl}$ for the possible rotation around the C1,C1′- and the C6,C1‴-axis were calculated using B3LYP/6-31G*. The simulations provided four possible geometries of (6*M*)-TS_{Aryl}-**6a** (TS_{1-1}–TS_{1-4}, Figure S22 in Supporting Information). In all of them the C1-linked aryl substituent possessed a nearly planar orientation toward the central aromatic ring. Since the interconversion of (1*M*,6*M*)-**6a** → (1*P*,6*M*)-**6a** is most likely to take place via TS_{1-1}—the lowest possible transition state—the calculation led to a rotational barrier of $\Delta G^{\ddagger}_{(1M,6M)\rightarrow(1P,6M)\text{-}\mathbf{6a}}$ = 129.6 kJ mol^{-1}. For the imaginable isomerization at the C6,C1‴-axis only two possible structures of (1*M*)-$TS_{Naphthyl}$-**6a** were obtained (TS_{2-1} and TS_{2-2}, S22 in Supporting Information), due to the already more space-demanding arrangement in the attempt to reach a planar orientation of the naphthyl moiety in relation to the central ring. The rotational barrier for the interconversion of the second pair of atropo-diastereomers was predicted to be $\Delta G^{\ddagger}_{(1M,6M)\rightarrow(1M,6P)\text{-}\mathbf{6a}}$ = 101.4 kJ mol^{-1}. These results showed that both biaryl axes are rotationally stable at room temperature. This is in agreement with the observed chromatographic resolution of the atropisomeric products. Since the reaction temperature does not exceed room temperature, one may expect that the observed atropisomeric product ratio is the result of a kinetically controlled reaction, not a thermodynamically controlled one.

After the successful synthesis, chiral resolution, and absolute configurational assignment of 1,2-type axially chiral naphthalene-substituted biphenyls, we focused our attention on the even more complicated and challenging 1,3-type axially chiral terphenyl scaffolds of type **9**. To prepare such 1,3-axially chiral terphenyls, the required starting material **8** was prepared conveniently and in high yield, by reaction of **2** with the phenylacetone **7**, following Tominaga's protocol as discussed earlier in Table 1.[42] The synthesis of the 4′-naphthalene-substituted terphenyls **9a**–**c** was achieved in 60–70% yields, by stirring an equimolar mixture of the pyranone **8**, the substituted phenylacetones **5a**–**c**, and powdered KOH in DMF for 10–12 h at room temperature (Table 3). The transformation of the 2*H*-pyran-2-one **8** to the naphthalene-substituted terphenyls **9a**–**c** is possibly initiated by a Michael addition of the conjugate base of substituted phenylacetones **5a**–**c** (generated by deprotonation at C1′) at position C6 of the respective lactone **8**, similar to the reaction mechanism shown in Table 1. Briefly, for the synthesis of naphthalene substituted terphenyl **9a**, stirring of an equimolar mixture of 6-(4-methoxyphenyl)-4-

Table 3. Synthetic Pathway to the Naphthalene Substituted Functionalized Terphenyls 9a–c

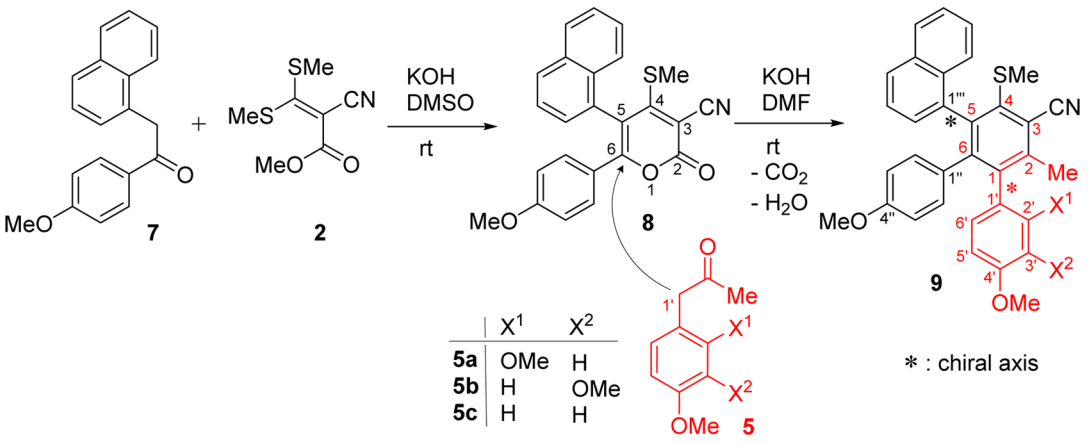

entry	X^1	X^2	time, h	yield, %
9a	OMe	H	12	60
9b	H	OMe	10	68
9c	H	H	10	70

DOI: 10.1021/acs.joc.6b01804
J. Org. Chem. 2016, 81, 10721–10732

(methylthio)-5-(naphthalen-1-yl)-2-oxo-2*H*-pyran-3-carbonitrile (**8**) and the 2,4-dimethoxy-phenylacetone (**5a**) at room temperature in the presence of powdered KOH in dry DMF gave 2′,4′,4″-trimethoxy-2-methyl-4-methylsulfanyl-5-(naphthalen-1‴-yl)[1,1′;6,1″]-terphenyl-3-carbonitrile (**9a**) in 60% yield, as a mixture of atropo-diastereomers in the ratio of 64:36 as calculated by the ^{1}H NMR peaks of the methyl and methoxy substituents.

All of the naphthalene-substituted terphenyls **9a–c** were characterized by spectroscopic analysis. The constitution of one of the products, *rac*-**9a**, was unambiguously confirmed by single-crystal X-ray analysis. The ^{1}H NMR spectrum of the (racemic) naphthalene-substituted terphenyl **9a** revealed the presence of two atropo-diastereomers. In the crystals, by contrast, only one of the two possible diastereomers (*P*,*M*)-**9a** occurred, plus, as expected, its enantiomer (*M*,*P*)-**9a**, i.e., both with a relative *unlike*-configuration, as evidenced by X-ray diffraction analysis (Figure 4).

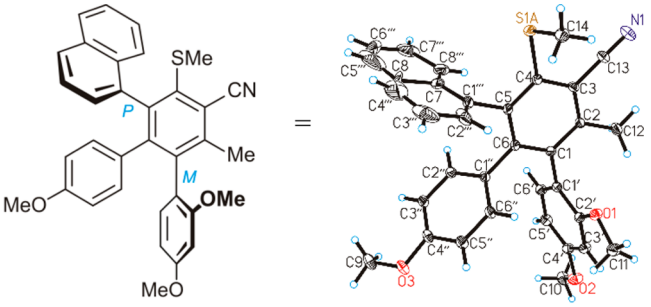

(1*M*,5*P*)-**9a**

Figure 4. Crystal structure (Oak Ridge Thermal-Ellipsoid Plot, ORTEP) of the *unlike* (1*M*,5*P*)-diastereomer of **9a** (CCDC No. 1487149). Likewise present in the crystal, but not shown, is the (1*P*,5*M*)-enantiomer. For the calculated structure of (1*M*,5*P*)-**9a**, see Table 4.

To investigate the as yet unknown absolute 1,3-type 2-fold axial chirality of this new class of naphthalene-substituted terphenyls, a method for the resolution of the respective atropisomers of **9a** was accomplished. When using a Phenomenex LUX cellulose 1 chiral-phase column (250 × 4.6 mm) at room temperature and a mixture of *n*-hexane/*i*-propanol (98:2) as the eluent at a flow rate of 1 mL min^{-1}, a resolution into two peaks (Figure S18, Peak A and Peak B in Supporting Information) was achieved in a nearly 82:18 ratio—instead of the expected four peaks. The ^{1}H NMR spectrum of **9a** had revealed that two atropo-diastereomers are present in a 64:36 ratio (i.e., four atropisomers in the ratio of 32:32:18:18), which suggested that the slower-eluting peak (peak B) was a pure atropisomer (i.e., enantio- and diastereomerically pure). In spite of several attempts on normal-phase chiral HPLC conditions even at low temperature, the separation of the atropisomers from peak A was unsuccessful on this phase. Even the serial connection of two identical Chiracel OD-RH columns (150 × 4.6 mm), using the following reverse phase chromatographic conditions: ambient temperature, H_2O/MeCN (35:65), flow rate = 1 mL min^{-1} resulted in an improved but still only partial resolution of the four possible atropisomers of *rac*-**9a**. The three peaks (30:50:20 ratio) were then investigated by online HPLC-UV and -CD spectroscopy in the stopped-flow mode (Figure 5).

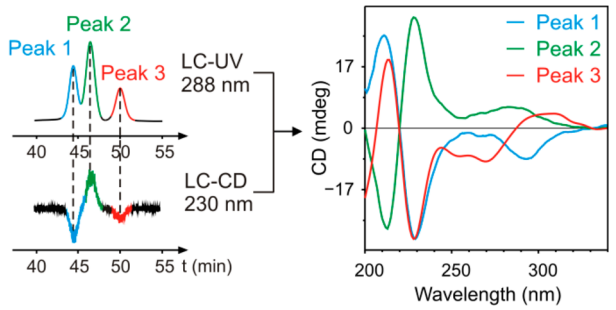

Figure 5. LC-UV and LC-CD traces of the resolved Peaks 1, 2, and 3, and their online ECD spectra.

The received ratio of 30:50:20 suggested that the two pairs of atropo-diastereomers occurred in a 1.5:1 ratio and that, thus, Peak 2 consisted of a mixture of stereoisomers. Due to the experimental CD spectrum they should be diastereomers instead of enantiomers, which otherwise would have canceled out each other's CD effects. In order to determine the absolute configuration of these atropisomers, a comparison of the experimental CD spectra and the computational CD spectra, obtained by quantum-chemical CD calculations, was essential. Despite the existing X-ray structure, full conformational analyses for the two sets of atropisomers—(1*M*,5*P*)- and (1*P*,5*P*)-**9a**—needed to be carried out due to the fact that the experimental CD spectra were measured in solution (Table 4

Table 4. Characteristic Dihedral Angles for All the Flexible Parts of 9a, Arbitrarily Depicted for the Minimum Structure of (1*M*,5*P*)-9a[a]

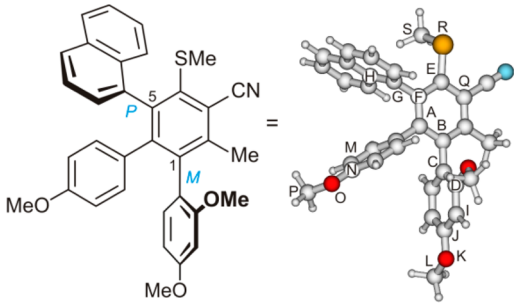

(1*M*,5*P*)-**9a**

θ_{ABCD}		θ_{EFGH}	θ_{IJKL}	θ_{MNOP}	θ_{QESR}
(1*P*) 75	(1*M*) −111	95	−180	180	64
(1*P*) 105	(1*M*) −62	83	0	0	−71

[a]For the crystal structure of (1*M*,5*P*)-**9a**, see Figure 4.

and further details in Supporting Information). The comparison of the conformation derived from the X-ray analysis with the ones calculated by different functionals (Table S4 in the Supporting Information) and the obtained RMSD (root-mean-square deviation) values led to B3LYP/6-31G* as the optimization method of choice, giving the best agreement with the X-ray structure (0.20 Å).

Optimization and subsequent single-point energy calculations (RI-SCS-MP2/def2-TZVP//COSMO: H_2O/MeCN: 35/65) of the 32 possible conformers (for each of the two diastereomers!) yielded 16 relevant structures for the (1*P*,5*P*)-isomer of **9a** and eight for its (1*M*,5*P*)-configured diastereomer. TDDFT calculations were carried out using the double-hybrid

DOI: 10.1021/acs.joc.6b01804
J. Org. Chem. 2016, 81, 10721−10732

functional B2PLYP in combination with the TZVP basis set and COSMO. After Boltzmann weighting and application of a UV correction of 7 nm (Figure S21 in Supporting Information), the obtained overall CD spectra were compared with the experimental curves and the similarity factors Σ_{fg} and the Δ_{ESI} values were determined (Table 5). Unfortunately, the

Table 5. CD Spectra, Similarity Factors (Σ_{fg}), and ESI Values in % for All Possible Stereoisomers of 9a Compared to Those of Peaks 1 and 3, Regarding the Wavelength Range of 190−400 nm for TDAB2PLYP and of 250−350 nm in the Case of RICC2 (Highlighted in Grey)

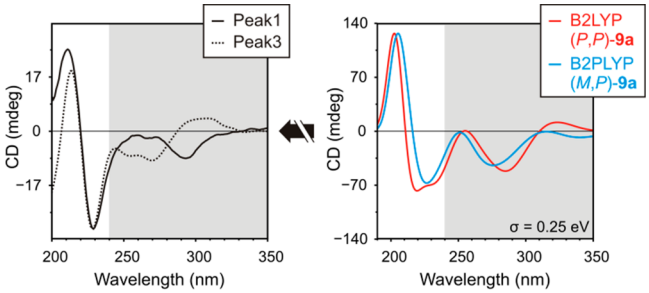

method	config.	Σ_{fg} Peak 1	Δ_{ESI} Peak 1	Σ_{fg} Peak 3	Δ_{ESI} Peak 3
B2PLYP	1*M*,5*P*	87	86	72	64
	1*P*,5*M*	0.7		8	
	1*P*,5*P*	92	91	70	58
	1*M*,5*M*	0.3		11	
RICC2	1*M*,5*P*	94	85	30	27
	1*P*,5*M*	9		56	
	1*P*,5*P*	18	44	89	89
	1*M*,5*M*	62		0.4	

CD spectra calculated for the two regarded atropo-diastereomers displayed almost identical curves and, thus, similarity factors Σ_{fg} for their comparison with the experimental CD spectra (depicted in Table 5 for Peaks 1 and 3).

Further investigations thus, necessarily, concentrated on the wavelength range of 250−350 nm, since only in this region the experimental CD behavior of Peaks 1 and 3 showed substantial differences, namely mirror-image like shaped curves (Table 5, highlighted in gray). In order to find the reason for the failure of the TD calculations to reproduce this particular experimental CD behavior, in-depth analyses of the excited states responsible for this wavelength region had to be carried out. For the evaluation of TD methods, Le Bahers and Ciofini et al.[43,44] have recently introduced the indices D_{CT}, t, and the spatial overlap $C_+(r)/C_-(r)$ (in the following referred to as ϑ). These indices can be used as a diagnostic tool to identify "pathologic" excited states, i.e., long-range charge-transfer (CT) transitions in the TD calculations (further details are described in Supporting Information). The investigation of the single excitations showed that in the case of the (1*M*,5*P*)-configured isomer three, and for (1*P*,5*P*)-**9a** even six states implied through-space CT transitions and were, thus, considered to be deficient ($t \geq 1.6$ Å and $\vartheta \leq 0.35$, Tables S11 and S13 in Supporting Information).

Even though the B2PLYP calculations were not applicable to the determination of the absolute configuration, they gave a first indication for the predominance of the naphthalene axis on the CD behavior in the lower wavelength region, meaning that Peaks 1 and 3 both possessed the same configuration at this axis, namely 5*P*.

In order to reassess the results obtained by the TD calculations, RICC2/def2-SV(P) coupled-cluster simulations for the first ten excited states based on the global minima of each of the two diastereomeric configurations (1*P*,5*P* and 1*M*,5*P*) were carried out to cover the wavelength range in question. For both diastereomeric configurations, all ten calculated excitations were indeed found to be local ones ($\vartheta \geq 0.78$, $t \ll 1.6$ Å, Tables S12 and S14 in Supporting Information) instead of the wrongly predicted through-space CT transitions in the B2PLYP calculations. Such erroneous transitions also affect the simulated CD behavior and can lead to a falsified line-shape Gaussian curve. As an example, the excitation at 296 nm, ns = 5 (B2PLYP, 4*P*,6*P*-**9a**), one of the artificial CT transitions, displayed a negative rotatory strength R = − 10 cgs, while the RICC2 simulation predicted a local excitation with a rather high positive rotatory strength R = +29 cgs at the same wavelength (ns = 3 at 297 nm). The "pathologic" excited states in the TD calculations are probably the reason for the indistinguishable overall CD curves calculated for the two atropo-diastereomers (1*P*,5*P*)- and (1*M*,5*P*)-**9a**.

By comparison of the UV and CD spectra from the RICC2 calculations with the experimental ones, the determination of the absolute configurations was possible now due to the more accurate description of the CD signals in the critical wavelength region, which was essential for a differentiation between the atropo-diastereomers of compound **9a** (Figure 6 and Figure S21 in Supporting Information for the UV shift). Not only the visual agreement, but also the calculated similarity factors (Σ_{fg}) and Δ_{ESI} values corroborated the determination of the first-eluting diastereomer as (1*M*,5*P*)-**9a** and the slowest-eluting one as (1*P*,5*P*)-**9a** (Table 5). Furthermore, the CD spectrum calculated for a mixture of the remaining configurations (1*M*,5*M*)- and (1*P*,5*M*)-**9a** showed a good agreement with the experimental one of Peak 2, leading to the assignment of the atropo-diastereomers of **9a** within the limits of the accomplished experimental resolution.

The dynamics of a possible interconversion of the atropo-diastereomers of **9a** by rotation around the C1,C1′ or the C5,C1‴ axes were investigated in the same way as already shown for **6a**. The simulations provided again four geometries of (5*M*)-TS_{Aryl}-**9a** (TS_{1-1}−TS_{1-4}, Figure S22 in Supporting Information). But in contrast to **6a**, the calculations for the isomerization at the naphthyl axis led to four structures of (1*M*)-$TS_{Naphthyl}$-**9a** (TS_{2-1}−TS_{2-4}, Figure S22 in Supporting Information). The interconversion pathway via the energetic most favorable transition states TS_{1-1} and TS_{2-1} yielded estimated barriers of $\Delta G^{\ddagger}_{(1M,5M)\rightarrow(1P,5M)\text{-}\mathbf{9a}}$ = 136.6 kJ mol^{-1} and $\Delta G^{\ddagger}_{(1M,5M)\rightarrow(1M,5P)\text{-}\mathbf{9a}}$ = 164.4 kJ mol^{-1} proving again that both investigated biaryl axes in **9a** are in fact rotationally stable at ambient temperature, suggesting that the observed atropisomeric ratios result from a kinetically (not thermodynamically) controlled reaction.

CONCLUSION

In summary, we have demonstrated an efficient synthesis for the preparation of functionally congested, axially chiral naphthalene-substituted biphenyls and terphenyls having two stereogenic axes (1,2- or 1,3-type) in good yields, through enolate-induced ring transformation of 2*H*-pyran-2-ones and substituted phenyl acetones. The absolute configurations of the atropo-diastereomers of compound **6a** and—within the limits of chiral HPLC resolution—of compound **9a** as well were

DOI: 10.1021/acs.joc.6b01804
J. Org. Chem. 2016, 81, 10721−10732

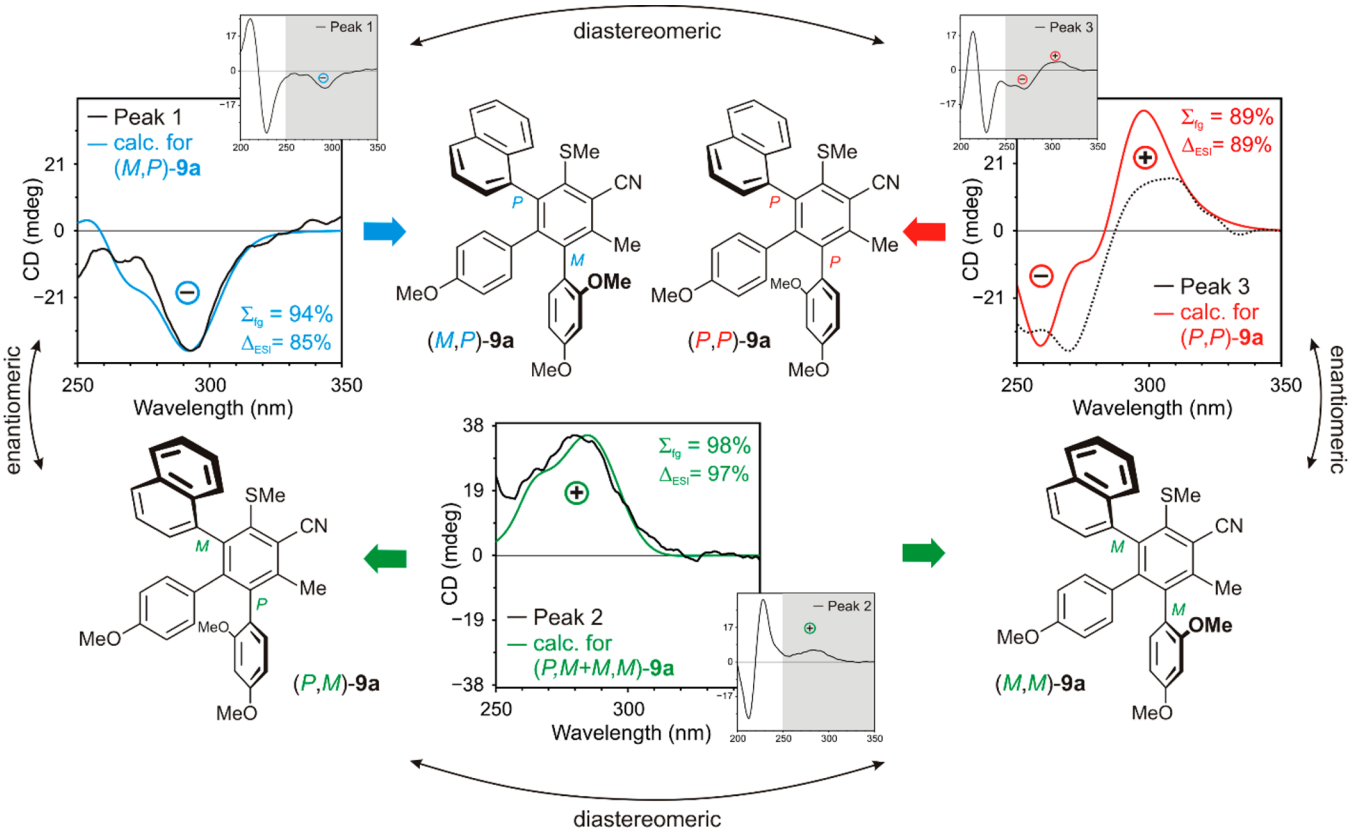

Figure 6. Assignment of the absolute configuration of the two diastereomers (1*M*,5*P*)- and (1*P*,5*P*)-**9a** and of the mixture containing (1*P*,5*M*)- and (1*M*,5*M*)-**9a**, by comparison of the experimental and the quantum-chemically calculated CD spectra using RICC2/def2-SV(P).

elucidated by the combination of NMR studies, online-HPLC experiments, electronic circular-dichroism (ECD) spectroscopy and quantum-chemical calculations. This synthetic approach offers—in a transition-metal-free environment—high flexibility in the construction of naphthalene-substituted bi- and terphenyls with the desired conformational freedom along the two molecular axes. The chosen experimental-computational strategy for the stereochemical investigation, as developed in this work, may help to characterize new axially chiral natural products with absolute configurations in a similar way and/or to develop new potential ligands for asymmetric synthesis. The work thus demonstrates the methodology for the synthesis and comprehensive stereochemical characterization of such crowded bi- and terphenyls in general.

EXPERIMENTAL SECTION

General Information. ^{1}H and ^{13}C NMR spectra were taken on a 300 MHz NMR instrument. Chemical shifts are reported in parts per million (ppm) relative to internal Me_4Si (δ 0 ppm for ^{1}H) or based on the central peak of the solvent $CDCl_3$ (δ 7.26 ppm for ^{1}H NMR and δ 77.00 ppm for ^{13}C NMR). Splitting patterns are indicated as s (singlet), d (doublet), dd (double of doublet), t (triplet), or m (multiplet). The minor and major diastereomers are represented as mnd and mjd, respectively. Coupling constants (J) are given in Hertz (Hz). Infrared (IR) spectra were taken in a KBr disc and are reported in wave numbers (cm^{-1}). MS (ESI) and HRMS (ESI) were recorded on a mass spectrophotometer with a Quadrupole Time-of-Flight (Q-TOF) mass analyzer. All reactions were carried out under anhydrous conditions and were monitored by TLC, visualization was done with UV light (254 nm).

Online HPLC and CD Experiments. All offline UV spectra were obtained at room temperature in *n*-hexane/2-propanol (1:1) with a UV spectrophotometer. The HPLC-CD spectra were recorded with an HPLC system equipped with a motor valve (PU-1580 pump, LG-980−02S gradient unit, MD-2010-DAD detector and a spectropolarimeter) at ambient temperature in the stopped-flow mode using a 5 mm standard flow cell and a scanning speed of 500 nm min^{-1}, with a response time of 0.5 s and a bandwidth of 0.5 nm (three repetition cycles).

The chiral resolution of biphenyl **6a** was achieved by the serial connection of two identical Chiracel OD-RH columns (150 × 4.6 mm, 5 μ) under reversed-phase chromatographic conditions with water−acetonitrile (15:85, v/v) as the mobile phase (both treated with 0.05% trifluoroacetic acid) at a flow rate of 0.5 mL min^{-1} at ambient temperature, leading to four baseline-separated peaks of atropisomers. Similarly the partial resolution of the four possible atropisomers of terphenyl **9a** was done by the serial connection of two identical Chiracel OD-RH columns (150 × 4.6 mm, 5 μ) under reversed-phase chromatographic conditions with water−acetonitrile (35:65, v/v) as the mobile phase at a flow rate of 1 mL min^{-1} at ambient temperature. No further improvement in the separation could be achieved by changing the HPLC conditions.

Computational Details. The conformational analyses for compounds **6a** and **9a** were carried out with the Gaussan09 program[45] using the B3LYP[46] functional in combination with Pople's 6-31G* basis set.[47] All of the subsequent calculations were based on these optimized structures. Single TDDFT excited-state calculations with the double-hybrid functional B2PLYP[48] in combination with Ahlrich's TZVP basis set[49] and the COSMO model[50] to include solvent effects as well as the single-point energy calculations were carried using the ORCA software package.[51] Coupled-cluster excitations for the atropodiastereomers of **6a** and **9a** were carried out with the Turbomole[52] software package using the RICC2/def2-SV(P) method.[53,54] The software SpecDis 1.60[39] was used to sum up single UV and CD spectra with corresponding oscillator (f in au) and rotational strength values (R in cgs (10^{-40} erg esu cm Gauss^{-1})) from the length formalism, for generation of line-shape Gaussian curves, UV correction[55] (B2PLYP = **6a**: 7 nm, **9a**: 7 nm; RICC2 = **6a**: 30 nm, **9a**: 34 nm), the comparison

DOI: 10.1021/acs.joc.6b01804
J. Org. Chem. 2016, 81, 10721−10732

with the experimental data, and plotting of the results. Harmonic vibrational frequencies were calculated with B3LYP/6-31G* for all of the stationary points used in the calculation of the inversion barriers. For each optimized ground state, frequency analysis verified the absence of any imaginary frequencies, whereas each transition state showed only one imaginary frequency. Visual inspection of the corresponding normal mode confirmed that the correct transition state had been identified.

General Procedure for the Synthesis of Naphthalene-Substituted Biphenyls (6a–f). A mixture of 6-(naphthalen-1-yl)-2-oxo-4-(piperidin-1-yl)-2*H*-pyran-3-carbonitriles (**4a**,**b**, 1 mmol, 1 equiv) and the substituted phenylacetones (**5a–c**, 1.2 equiv) and powdered KOH (1.2 equiv) in dry DMF (5 mL) was stirred at room temperature for 6–9 h. The progress of the reaction was monitored by TLC. On completion, the solvent was evaporated and the reaction mixture was poured onto crushed ice with vigorous stirring and finally neutralized with 10% HCl. The precipitate obtained was filtered and purified on a silica gel column using 10% ethyl acetate in *n*-hexane as the eluent to afford a mixture of atropo-diastereomers of **6a–f** as a white solid.

*2′, 4′-Dimethoxy-2-methyl-4-(piperidin-1″-yl)-6-(naphthalen-1‴-yl)biphenyl-3-carbonitrile (**6a**).* White solid (51:49 mixture of atropo-diastereomers) **6a** (347 mg, 75% yield); R_f = 0.51 (*n*-hexane/ethyl acetate, 4:1, v/v); mp (*n*-hexane/ethyl acetate) 168–170 °C; MS (ESI) 463 [M + H$^+$]; IR (KBr) ν = 2932 (s), 2849 (w), 2213 (s), 1580 (s), 1509 (w), 1456 (s) cm^{-1}; ^{1}H NMR (300 MHz, $CDCl_3$) δ = 1.54–1.62 (m, 4H, mix of mnd and mjd), 1.74–1.82 (m, 8H, mix of mnd and mjd), 2.29 (s, 3H, mnd), 2.34 (s, 3H, mjd), 3.12–3.18 (m, 11H, mix of mnd and mjd), 3.61 (s, 3H, mnd), 3.64 (s, 3H, mjd), 3.74 (s, 3H, mnd), 5.96–6.04 (m, 2H, mix of mnd and mjd), 6.18–6.30 (m, 2H, mix of mnd and mjd), 6.47 (d, J = 8.3 Hz, 1H, mnd), 6.78 (d, J = 8.3 Hz, 1H, mjd), 6.86–6.90 (m, 2H, mix of mnd and mjd), 7.07–7.10 (m, 2H, mix of mnd and mjd), 7.20–7.46 (m, 6H, mix of mnd and mjd), 7.61–7.79 (m, 6H, mix of mnd and mjd) ppm; ^{13}C NMR (75 MHz, $CDCl_3$) δ = 19.4, 19.6, 24.1, 26.2, 53.5, 54.5, 55.1, 55.2, 97.8, 97.9, 103.6, 103.8, 106.6, 106.7, 118.2, 118.8, 118.9, 119.7, 120.4, 124.4, 124.7, 125.1, 125.4, 125.8, 125.9, 126.0, 126.6, 127.1, 127.2, 127.3, 127.7, 128.1, 130.6, 131.6, 131.8, 132.1, 132.2, 133.1, 133.2, 139.0, 139.1, 143.4, 143.7, 145.7, 146.1, 155.5, 155.7, 157.3, 157.6, 159.6, 160.0 ppm; HRMS (ESI) calculated for $C_{31}H_{31}N_2O_2$ [M + H$^+$] 463.2386, found 463.2366.

*3′,4′-Dimethoxy-2-methyl-4-(piperidin-1″-yl)-6-(naphthalen-1‴-yl)biphenyl-3-carbonitrile (**6b**).* White solid (60:40 mixture of atropo-diastereomers) **6b** (370 mg, 80% yield); R_f = 0.44 (*n*-hexane/ethyl acetate, 4:1, v/v); mp (*n*-hexane/ethyl acetate) 185–187 °C; MS (ESI) 463 [M + H$^+$]; IR (KBr) ν = 2928 (s), 2795 (m), 2214 (s), 1582 (m), 1517 (m), 1451 (s) cm^{-1}; ^{1}H NMR (300 MHz, $CDCl_3$) δ = 1.53–1.63 (m, 4H, mix of mnd and mjd), 1.74–1.84 (m, 8H, mix of mnd and mjd), 2.41 (s, 6H, mix of mnd and mjd), 3.05 (s, 3H, mjd), 3.12–3.22 (m, 8H, mix of mnd and mjd), 3.67 (s, 6H, mix of mnd and mjd), 3.73 (s, 3H, mnd), 6.14 (br s, 1H, mjd), 6.32–6.70 (m, 5H, mix of mnd and mjd), 6.89 (br s, 2H, mix of mnd and mjd), 6.96–7.02 (m, 1H, mjd), 7.13–7.48 (m, 7H, mix of mnd and mjd), 7.49–7.81 (m, 6H, mix of mnd and mjd) ppm; ^{13}C NMR (75 MHz, $CDCl_3$) δ = 19.9, 24.0, 26.1, 53.3, 54.9, 55.5, 55.7, 106.8, 110.1, 110.3, 112.7, 113.8, 117.9, 118.5, 118.7, 122.0, 122.3, 124.5, 124.8, 125.4, 125.7, 125.8, 125.9, 126.0, 126.9, 127.3, 127.5, 127.9, 128.1, 131.0, 131.1, 131.5, 132.0, 133.1, 135.4, 135.5, 138.8, 142.2, 145.3, 147.4, 147.7, 155.7 ppm; HRMS (ESI) calculated for $C_{31}H_{31}N_2O_2$ [M + H$^+$] 463.2386, found 463.2359.

*4′-Methoxy-2-methyl-4-(piperidin-1″-yl)-6-(naphthalen-1‴-yl)-biphenyl-3-carbonitrile (**6c**).* White solid (390 mg, 90% yield); R_f = 0.58 (*n*-hexane/ethyl acetate, 4:1, v/v); mp (*n*-hexane/ethyl acetate) 158–160 °C; MS (ESI) 433 [M + H$^+$]; IR (KBr) ν = 2934 (s), 2798 (m), 2210 (s), 1581 (s), 1511 (m), 1451 (s) cm^{-1}; ^{1}H NMR (300 MHz, $CDCl_3$) δ = 1.52–1.61 (m, 2H), 1.74–1.82 (m, 4H), 2.36 (s, 3H), 3.08–3.24 (m, 4H), 3.62 (s, 3H), 6.39 (d, J = 6.6 Hz, 1H), 6.64 (d, J = 8.3 Hz, 2H), 6.86 (s, 1H), 6.94 (d, J = 8.3 Hz, 1H), 7.06 (d, J = 6.9 Hz, 1H), 7.23–7.29 (m, 1H), 7.36–7.40 (m, 2H), 7.56 (d, J = 8.5 Hz, 1H), 7.66 (d, J = 8.2 Hz, 1H), 7.76 (d, J = 7.3 Hz, 1H) ppm; ^{13}C NMR (75 MHz, $CDCl_3$) δ = 20.0, 24.0, 26.2, 53.4, 54.9, 106.8, 112.9, 118.0, 118.8, 124.6, 125.5, 125.8, 126.0, 127.2, 127.3, 128.0, 130.3, 130.8, 131.2, 131.7, 133.1, 135.5, 138.8, 142.4, 145.3, 155.7, 157.9 ppm; HRMS (ESI) calculated for $C_{30}H_{29}N_2O$ [M + H$^+$] 433.2280, found 433.2267.

*2′,4′-Dimethoxy-2-methyl-4-(4″-methylpiperidin-1″-yl)-6-(naphthalen-1‴-yl)biphenyl-3-carbonitrile (**6d**).* White solid (51:49 mixture of atropo-diastereomers) **6d** (372 mg, 78% yield); R_f = 0.52 (*n*-hexane/ethyl acetate, 4:1, v/v); mp (*n*-hexane/ethyl acetate) 164–166 °C; MS (ESI) 477 [M + H$^+$]; IR (KBr) ν = 2933 (s), 2848 (w), 2213 (s), 1580 (s), 1509 (w), 1456 (s) cm^{-1}; ^{1}H NMR (300 MHz, $CDCl_3$) δ = 0.95–1.04 (m, 6H, mix of mnd and mjd), 1.49–1.62 (m, 6H, mix of mnd and mjd), 1.68–1.76 (m, 4H, mix of mnd and mjd), 2.29 (s, 3H, mnd), 2.34 (s, 3H, mjd), 2.72–2.82 (m, 4H, mix of mnd and mjd), 3.20 (s, 3H, mjd), 3.54–3.64 (m, 10H, mix of mnd and mjd), 3.74 (s, 3H, mnd), 5.95–6.02 (m, 2H, mix of mnd and mjd), 6.19–6.30 (m, 2H, mix of mnd and mjd), 6.47 (d, J = 8.3 Hz, 1H, mnd), 6.78 (d, J = 8.3 Hz, 1H, mjd), 6.86–6.90 (m, 2H, mix of mnd and mjd), 7.06–7.10 (m, 2H, mix of mnd and mjd), 7.20–7.46 (m, 6H, mix of mnd and mjd), 7.61–7.78 (m, 6H, mix of mnd and mjd) ppm; ^{13}C NMR (75 MHz, $CDCl_3$) δ = 19.4, 19.6, 21.8, 30.6, 34.5, 52.6, 52.9, 53.0, 54.5, 55.1, 55.2, 97.8, 97.9, 103.5, 103.8, 106.5, 106.6, 118.2, 118.8, 118.9, 119.7, 120.4, 124.4, 124.7, 125.1, 125.4, 125.8, 125.9, 126.0, 126.6, 127.1, 127.2, 127.3, 127.7, 128.1, 130.6, 131.5, 131.8, 132.2, 133.1, 139.0, 139.1, 143.4, 143.7, 145.7, 146.1, 155.3, 155.5, 157.3, 157.6, 159.9, 160.0 ppm; HRMS (ESI) calculated for $C_{32}H_{33}N_2O_2$ [M + H$^+$] 477.2542, found 477.2533.

*3′,4′-Dimethoxy-2-methyl-4-(4″-methylpiperidin-1″-yl)-6-(naphthalen-1‴-yl)biphenyl-3-carbonitrile (**6e**).* White solid (60:40 mixture of atropo-diastereomers) **6e** (405 mg, 85% yield); R_f = 0.46 (*n*-hexane/ethyl acetate, 4:1, v/v); mp (*n*-hexane/ethyl acetate) 148–150 °C; MS (ESI) 477 [M + H$^+$]; IR (KBr) ν = 2917 (s), 2842 (w), 2812 (m), 2210 (s), 1581 (s), 1513 (m), 1452 (s) cm^{-1}; ^{1}H NMR (300 MHz, $CDCl_3$) δ = 0.96–1.04 (m, 6H, mix of mnd and mjd), 1.49–1.62 (m, 6H, mix of mnd and mjd), 1.68–1.76 (m, 4H, mix of mnd and mjd), 2.41 (s, 6H, mix of mnd and mjd), 2.74–2.80 (m, 4H, mix of mnd and mjd), 3.04 (s, 3H, mjd), 3.52–3.75 (m, 13H, mix of mnd and mjd), 6.14 (s, 1H, mix of mnd and mjd), 6.34–6.65 (m, 5H, mix of mnd and mjd), 6.90–6.7.01 (m, 3H, mix of mnd and mjd), 7.11–7.51 (m, 7H, mix of mnd and mjd), 7.53–7.80 (m, 6H, mix of mnd and mjd), ppm; ^{13}C NMR (75 MHz, $CDCl_3$) δ = 20.0, 21.8, 30.6, 34.4, 34.5, 52.5, 53.0, 55.0, 55.5, 106.8, 110.1, 110.2, 112.7, 113.8, 118.0, 118.6, 118.8, 122.1, 122.3, 124.8, 125.5, 125.8, 125.9, 126.9, 127.4, 128.0, 128.2, 131.1, 132.1, 133.1, 135.6, 138.8, 142.3, 145.4, 147.4, 147.7, 155.5 ppm; HRMS (ESI) calculated for $C_{32}H_{33}N_2O_2$ [M + H$^+$] 477.2542, found 477.2541.

*4′-Methoxy-2-methyl-4-(4″-methylpiperidin-1″-yl)-6-(naphthalen-1‴-yl)biphenyl-3-carbonitrile (**6f**).* White solid (410 mg, 92% yield); R_f = 0.56 (*n*-hexane/ethyl acetate, 4:1, v/v); mp (*n*-hexane/ethyl acetate) 178–180 °C; MS (ESI) 447 [M + H$^+$]; IR (KBr) ν = 2939 (s), 2808 (w), 2213 (s), 1584 (s), 1517 (s), 1456 (s) cm^{-1}; ^{1}H NMR (300 MHz, $CDCl_3$) δ = 1.00 (d, J = 4.9 Hz, 3H), 1.52–1.62 (m, 3H), 1.68–1.77 (m, 2H), 2.36 (s, 3H), 2.72–2.79 (m, 2H), 3.55–3.65 (m, 5H), 6.40 (d, J = 8.5 Hz, 1H), 6.64 (d, J = 7.7 Hz, 2H), 6.87 (s, 1H), 6.94 (d, J = 9.3 Hz, 1H), 7.07 (d, J = 7.0 Hz, 1H), 7.25–7.29 (m, 1H), 7.36–7.42 (m, 2H), 7.56 (d, J = 7.5 Hz, 1H), 7.66 (d, J = 8.2 Hz, 1H), 7.74–7.78 (m, 1H) ppm; ^{13}C NMR (75 MHz, $CDCl_3$) δ = 20.1, 21.8, 30.6, 34.4, 34.5, 52.5, 53.0, 54.9, 106.8, 113.0, 118.0, 118.9, 124.7, 125.5, 125.8, 126.0, 127.2, 127.4, 128.1, 130.3, 130.9, 131.2, 131.7, 133.2, 135.5, 138.8, 142.5, 145.3, 155.4, 158.0 ppm; HRMS (ESI) calculated for $C_{31}H_{31}N_2O$ [M + H$^+$] 447.2436, found 447.2425.

*6-(4-Methoxyphenyl)-4-methylsulfanyl-5-naphthalen-1-yl-2-oxo-2H-pyran-3-carbonitrile (**8**).* A mixture of methyl 2-cyano-3,3-dimethylsulfanyl acrylate (**2**, 1 mmol, 1 equiv), the 1-(4-methoxyphenyl)-2-naphthalen-1-yl-ethanone (**7**, 1.2 mmol, 1.2 equiv) and powdered KOH (1.2 mmol, 1.2 equiv) in dry DMSO (5 mL) was stirred at room temperature for 18 h. The progress of the reaction was monitored by TLC and on completion, reaction mixture was poured onto crushed ice with vigorous stirring. The precipitate obtained was filtered and purified on a silica gel column to afford 6-(4-

DOI: 10.1021/acs.joc.6b01804
J. Org. Chem. 2016, 81, 10721–10732

methoxyphenyl)-4-methylsulfanyl-5-naphthalen-1-yl-2-oxo-2*H*-pyran-3-carbonitrile (**8**). Yellow solid; (340 mg, 85% yield); R_f = 0.55 (chloroform/methanol, 99:1, v/v); mp (chloroform/methanol) 158−160 °C; MS (FAB) 400 [M + H]$^+$; IR (KBr) ν = 1718 (s), 2214 (s) cm^{-1}; ^{1}H NMR (200 MHz, $CDCl_3$) δ 2.73 (s, 3H), 3.68 (s, 3H), 6.54 (d, J = 9.0 Hz, 2H), 7.12 (d, J = 9.0 Hz, 2H), 7.26−7.32 (m, 1H), 7.42−7.56 (m, 3H), 7.61−7.70 (m, 1H), 7.88−8.00 (m, 2H); ^{13}C NMR (100 MHz, DMSO-d_6) δ = 18.0, 55.7, 93.0, 114.1, 115.5, 116.2, 123.7, 125.3, 126.2, 126.9, 127.6, 129.0, 130.0, 130.2, 130.8, 130.9, 132.7, 133.6, 157.9, 159.0, 161.5, 171.4 ppm; HRMS calculated for $C_{24}H_{18}NO_3S$ [M + H$^+$] 400.1007, found 400.1001.

General Procedure for the Synthesis of Naphthalene-Substituted Biphenyls (9a−c). A mixture of 6-(4-methoxyphenyl)-4-(methylthio)-5-(naphthalen-1-yl)-2-oxo-2*H*-pyran-3-carbonitrile (**8**, 1 mmol, 1 equiv), the 2,4-dimethoxy-phenylacetone (**5a**, 1.2 equiv) and powdered KOH (1.2 equiv) in dry DMF (5 mL) was stirred at room temperature for 10−12 h. The progress of reaction was monitored by TLC and on completion, solvent was evaporated and reaction mixture was poured onto crushed ice with vigorous stirring and finally neutralized with 10% HCl. The precipitate obtained was filtered and purified on a silica gel column using 20% ethyl acetate in *n*-hexane as the eluent to afford a mixture of atropo-diastereomers of **9a−c** as a white solid.

*2′,4′,4″-Trimethoxy-2-methyl-4-methylsulfanyl-5-(naphthalen-1‴-yl)[1,1′;6,1″]-terphenyl-3-carbonitrile (**9a**).* White solid (64:36 mixture of atropo-diastereomers) of **9a** (318 mg, 60% yield); R_f = 0.58 (*n*-hexane/ethyl acetate, 3:1, v/v); mp (*n*-hexane/ethyl acetate) 188−190 °C; MS (ESI$^+$) 532 [M$^+$+1]; IR (KBr) ν = 3019 (m), 2927 (s), 2853 (w), 2212 (m), 1610 (s), 1511 (s) cm^{-1}; ^{1}H NMR (300 MHz, $CDCl_3$) δ = 2.22 (s, 3H, mnd), 2.24 (s, 3H, mjd), 2.39 (s, 3H, mjd), 2.40 (s, 3H, mnd), 3.47 (s, 3H, mnd), 3.48 (s, 3H, mjd), 3.60 (s, 3H, mnd), 3.71 (s, 3H, mjd), 3.73 (br s, 6H, mix of mnd and mjd), 5.97−6.03 (m, 2H, mix of mnd and mjd), 6.24−6.42 (m, 8H, mix of mnd and mjd), 6.61−6.78 (m, 4H, mix of mnd and mjd), 7.00−7.14 (m, 2H, mix of mnd and mjd), 7.21−7.31 (m, 2H, mix of mnd and mjd), 7.35−7.50 (m, 6H, mix of mnd and mjd), 7.62−7.69 (m, 2H, mix of mnd and mjd), 7.73−779 (m, 2H, mix of mnd and mjd) ppm; ^{13}C NMR (100 MHz, DMSO-d_6) data could not be obtained due to poor solubility; HRMS calculated for $C_{34}H_{30}NO_3S$ [M + H$^+$] 532.1946, found 532.1940.

*3′,4′,4″-Trimethoxy-2-methyl-4-methylsulfanyl-5-(naphthalen-1‴-yl)[1,1′;6,1″]-terphenyl-3-carbonitrile (**9b**).* White solid (53:47 mixture of atropo-diastereomers) of **9b** (361 mg, 68% yield); R_f = 0.48 (*n*-hexane/ethyl acetate, 3:1, v/v); mp (*n*-hexane/ethyl acetate) 148−150 °C; MS (ESI) 532 [M + H$^+$]; IR (KBr) ν = 2925 (s), 2848 (w), 2217 (s), 1604 (m), 1514 (s), 1458 (m) cm^{-1}; ^{1}H NMR (300 MHz, $CDCl_3$) δ = 2.22 (s, 3H, mnd), 2.24 (s, 3H, mjd), 2.48 (s, 3H, mnd), 2.49 (s, 3H, mjd), 3.47 (s, 3H, mnd), 3.48 (s, 3H, mjd), 3.60 (s, 3H, mjd), 3.69 (s, 3H, mnd), 3.81 (s, 3H, mnd), 3.83 (s, 3H, mjd), 6.01−6.06 (m, 2H, mix of mnd and mjd), 6.28−6.48 (m, 6H, mix of mnd and mjd), 6.52−6.79 (m, 6H, mix of mnd and mjd), 6.99 (d, J = 6.9 Hz, 1H, mjd), 7.12 (d, J = 6.9 Hz, 1H, mnd), 7.21−7.50 (m, 8H, mix of mnd and mjd), 7.64−7.81 (m, 4H, mix of mnd and mjd) ppm; ^{13}C NMR (75 MHz, $CDCl_3$) δ = 20.2, 20.4, 54.7, 55.6, 55.7, 55.8, 110.4, 110.5, 111.7, 112.1, 112.3, 113.3, 113.4, 117.4, 118.9, 122.3, 124.5, 124.7, 125.5, 125.6, 125.7, 125.8, 125.9, 127.5, 127.6, 127.9, 128.1, 128.2, 128.3, 129.4, 130.0, 130.9, 131.0, 131.1, 131.2, 131.3, 132.2, 132.6, 132.8, 132.9, 137.0, 137.1, 139.6, 141.8, 141.9, 142.8, 142.9, 143.2, 146.7, 147.6, 148.2, 148.3, 157.4, 157.5 ppm; HRMS calculated for $C_{34}H_{30}NO_3S$ [M + H$^+$] 532.1946, found 532.1938.

*4′,4″-Dimethoxy-2-methyl-4-methylsulfanyl-5-(naphthalen-1‴-yl)[1,1′;6,1″]-terphenyl-3-carbonitrile (**9c**).* White solid (351 mg, 70% yield); R_f = 0.65 (*n*-hexane/ethyl acetate, 3:1, v/v); mp (*n*-hexane/ethyl acetate) 160−162 °C; MS (ESI) 502 [M + H$^+$]; IR (KBr) ν = 2924 (m), 2842 (w), 2219 (m), 1606 (s), 1510 (s), 1461 (w) cm^{-1}; ^{1}H NMR (300 MHz, $CDCl_3$) δ = 2.23 (s, 3H), 2.45 (s, 3H), 3.48 (s, 3H), 3.74 (s, 3H), 6.03−6.07 (m, 1H), 6.31−6.37 (m, 2H), 6.64 (d, J = 8.4 Hz, 1H), 6.68−6.78 (m, 2H), 6.85 (dd, J = 8.4, 1.8 Hz, 1H), 6.94 (dd, J = 8.3, 2.0 Hz, 1H), 7.07 (d, J = 6.4 Hz, 1H), 7.23−7.29 (m, 1H), 7.39−7.47 (m, 3H), 7.68 (d, J = 8.2 Hz, 1H), 7.76−7.79 (m, 1H) ppm; ^{13}C NMR (75 MHz, $CDCl_3$) δ = 20.3, 20.4, 54.7, 55.1, 111.9, 112.1, 113.3, 113.4, 117.5, 118.9, 124.7, 125.5, 125.7, 125.9, 127.6, 128.1, 128.3, 129.8, 130.8, 130.9, 131.1, 131.2, 132.5, 132.9, 137.1, 139.5, 142.1, 142.9, 143.2, 146.9, 157.4, 158.2 ppm; HRMS calculated for $C_{33}H_{28}NO_2S$ [M + H$^+$] 502.1840, found 502.1842.

■ ASSOCIATED CONTENT

Supporting Information

The Supporting Information is available free of charge on the ACS Publications website at DOI: 10.1021/acs.joc.6b01804.

Details of the stereochemical and computational analysis of **6a** and **9a** (including the Cartesian coordinates); copies of the ^{1}H and ^{13}C NMR spectra of the compounds **6a−f**, **9a−c** (PDF)

X-ray data (**9a**, CCDC No. 1487149) (CIF)

■ AUTHOR INFORMATION

Corresponding Authors

*Fax: +91(522)2771941. E-mail: atul_goel@cdri.res.in.

*Fax: +49(931)3184755. E-mail: bringman@chemie.uni-wuerzburg.de.

Notes

The authors declare no competing financial interest.

■ ACKNOWLEDGMENTS

Authors are thankful to the Council of Scientific and Industrial Research (CSIR), New Delhi, and to the Alexander-von-Humboldt Foundation, Germany, for financial support and research fellowships. The institutional communication number for the manuscript is 9336.

■ REFERENCES

(1) (a) Bringmann, G.; Price Mortimer, A. J.; Keller, P. A.; Gresser, M. J.; Garner, J.; Breuning, M. *Angew. Chem., Int. Ed.* **2005**, *44*, 5384. (b) Brunel, J. M. *Chem. Rev.* **2005**, *105*, 875. (c) Fernández-Pérez, H.; Etayo, P.; Panossian, A.; Vidal-Ferran, A. *Chem. Rev.* **2011**, *111*, 2119. (d) Noyori, R.; Takaya, H. *Acc. Chem. Res.* **1990**, *23*, 345.

(2) (a) Michl, J.; Sykes, E. C. H. *ACS Nano* **2009**, *3*, 1042. (b) Kottas, G. S.; Clarke, L. I.; Horinek, D.; Michl, J. *Chem. Rev.* **2005**, *105*, 1281.

(3) (a) Bringmann, G.; Gulder, T.; Gulder, T. A. M.; Breuning, M. *Chem. Rev.* **2011**, *111*, 563. (b) Ibrahim, S. R. M.; Mohamed, G. A. *Fitoterapia* **2015**, *106*, 194.

(4) (a) Hayashi, T.; Hayashizaki, K.; Ito, Y. *Tetrahedron Lett.* **1989**, *30*, 215. (b) Tsubaki, K.; Miura, M.; Nakamura, A.; Kawabata, T. *Tetrahedron Lett.* **2006**, *47*, 1241. (c) Zhang, Y.; Han, J.; Liu, Z.-J. *J. Org. Chem.* **2016**, *81*, 1317. (d) Faggi, E.; Sebastián, R. M.; Pleixats, R.; Vallribera, A.; Shafir, A.; Rodríguez-Gimeno, A.; de Arellano, C. R. *J. Am. Chem. Soc.* **2010**, *132*, 17980.

(5) (a) Mazzanti, A.; Chiarucci, M.; Bentley, K. W.; Wolf, C. *J. Org. Chem.* **2014**, *79*, 3725. (b) Ambrogi, M.; Ciogli, A.; Mancinelli, M.; Ranieri, S.; Mazzanti, A. *J. Org. Chem.* **2013**, *78*, 3709. (c) Nicolaou, K. C.; Boddy, C. N. C.; Bräse, S.; Winssinger, N. *Angew. Chem., Int. Ed.* **1999**, *38*, 2096. (d) Shibata, T.; Tsuchikama, K.; Otsuka, M. *Tetrahedron: Asymmetry* **2006**, *17*, 614.

(6) (a) Gunasekaran, P.; Perumal, S.; Menéndez, J. C.; Mancinelli, M.; Ranieri, S.; Mazzanti, A. *J. Org. Chem.* **2014**, *79*, 11039. (b) Quideau, S.; Feldman, K. S. *Chem. Rev.* **1996**, *96*, 475.

(7) Bringmann, G.; Günther, C.; Ochse, M.; Schupp, O.; Tasler, S. Axially Chiral Biaryls, a Multi-Facetted Class of Stereochemically, Biosynthetically, and Pharmacologically Intriguing Secondary Metabolites. In *Progr. Chem. Org. Nat. Prod.*; Herz, W., Falk, H., Kirby, G. W., Moore, R. E., Tamm, C., Eds.; Springer: Weinheim, 2001; Vol. *82*, p 1.

DOI: 10.1021/acs.joc.6b01804
J. Org. Chem. 2016, 81, 10721−10732

(8) Bringmann, G.; Pabst, T.; Henschel, P.; Kraus, J.; Peters, K.; Peters, E.-M.; Rycroft, D. S.; Connolly, J. D. *J. Am. Chem. Soc.* **2000**, *122*, 9127.
(9) Freedman, T. B.; Cao, X.; Oliveira, R. V.; Cass, Q. B.; Nafie, L. A. *Chirality* **2003**, *15*, 196.
(10) MacRae, W. D.; Towers, G. H. N. *Phytochemistry* **1984**, *23*, 1207.
(11) Dagne, E.; Steglich, W. *Phytochemistry* **1984**, *23*, 1729.
(12) Boyd, M. R.; Hallock, Y. F.; Cardellina, J. H., II; Manfredi, K. P.; Blunt, J. W.; McMahon, J. B.; Buckheit, R. W., Jr.; Bringmann, G.; Schäffer, M.; Cragg, G. M.; Thomas, D. W.; Jato, J. G. *J. Med. Chem.* **1994**, *37*, 1740.
(13) Bringmann, G.; Zagst, R.; Schäffer, M.; Hallock, Y. F.; Cardellina, J. H., II; Boyd, M. R. *Angew. Chem., Int. Ed. Engl.* **1993**, *32*, 1190.
(14) Bringmann, G.; Lombe, B. K.; Steinert, C.; Ioset, K. N.; Brun, R.; Turini, F.; Heubl, G.; Mudogo, V. *Org. Lett.* **2013**, *15*, 2590.
(15) Xu, M.; Bruhn, T.; Hertlein, B.; Brun, R.; Stich, A.; Wu, J.; Bringmann, G. *Chem. - Eur. J.* **2010**, *16*, 4206.
(16) Bringmann, G.; Zhang, G.; Büttner, T.; Bauckmann, G.; Kupfer, T.; Braunschweig, H.; Brun, R.; Mudogo, V. *Chem. - Eur. J.* **2013**, *19*, 916.
(17) Grilli, S.; Lunazzi, L.; Mazzanti, A.; Pinamonti, M. *Tetrahedron* **2004**, *60*, 4451.
(18) (a) Hassan, J.; Sévignon, M.; Gozzi, C.; Schulz, E.; Lemaire, M. *Chem. Rev.* **2002**, *102*, 1359. (b) Osako, T.; Uozumi, Y. *Org. Lett.* **2014**, *16*, 5866.
(19) (a) Bolm, C.; Hildebrand, J. P.; Muñiz, K.; Hermanns, N. *Angew. Chem., Int. Ed.* **2001**, *40*, 3284. (b) Gustafson, J. L.; Lim, D.; Barrett, K. T.; Miller, S. J. *Angew. Chem., Int. Ed.* **2011**, *50*, 5125.
(20) Goel, A.; Singh, F. V.; Dixit, M.; Verma, D.; Raghunandan, R.; Maulik, P. R. *Chem. - Asian J.* **2007**, *2*, 239.
(21) Goel, A.; Singh, F. V.; Kumar, V.; Reichert, M.; Gulder, T. A. M.; Bringmann, G. *J. Org. Chem.* **2007**, *72*, 7765.
(22) Dell'Erba, C.; Gasparrini, F.; Grilli, S.; Lunazzi, L.; Mazzanti, A.; Novi, M.; Pierini, M.; Tavani, C.; Villani, C. *J. Org. Chem.* **2002**, *67*, 1663.
(23) Walters, R. S.; Kraml, C. M.; Byrne, N.; Ho, D. M.; Qin, Q.; Coughlin, F. J.; Bernhard, S.; Pascal, R. A., Jr. *J. Am. Chem. Soc.* **2008**, *130*, 16435.
(24) (a) Tumambac, G. E.; Wolf, C. *J. Org. Chem.* **2004**, *69*, 2048. (b) Tumambac, G. E.; Wolf, C. *Org. Lett.* **2005**, *7*, 4045. (c) Mei, X.; Martin, R. M.; Wolf, C. *J. Org. Chem.* **2006**, *71*, 2854. (d) Lunazzi, L.; Mancinelli, M.; Mazzanti, A. *J. Org. Chem.* **2008**, *73*, 2198.
(25) (a) Roussel, C.; Kaid-slimane, R.; Andreoli, F.; Renaudin, M.; Vanthuyne, N. *Chirality* **2009**, *21*, 160. (b) Hîrtopeanu, A.; Suteu, C.; Uncuta, C.; Mihai, G.; Roussel, C. *Eur. J. Org. Chem.* **2000**, *2000*, 1081.
(26) (a) Bringmann, G.; Gulder, T. A. M.; Reichert, M.; Gulder, T. *Chirality* **2008**, *20*, 628. (b) Harada, N.; Nakanishi, K.; Berova, N. In *Applications in Stereochemical Analysis of Synthetic Compounds, Natural Products, and Biomolecules*, 1st ed.; Berova, N., Polavarapu, P. L., Nakanishi, K., Woody, R. W., Eds.; John Wiley & Sons, Inc.: Hoboken, NJ, 2012; Comprehensive Chiroptical Spectroscopy, Vol. 2, pp 115–166.
(27) (a) Freedman, T. B.; Cao, X.; Dukor, R. K.; Nafie, L. A. *Chirality* **2003**, *15*, 743. (b) Yang, G.; Xu, Y. *Top. Curr. Chem.* **2010**, *298*, 189. (c) Taniguchi, T.; Monde, K. *J. Am. Chem. Soc.* **2012**, *134*, 3695. (d) Taniguchi, T.; Manai, D.; Shibata, M.; Itabashi, Y.; Monde, K. *J. Am. Chem. Soc.* **2015**, *137*, 12191.
(28) He, Y.; Wang, B.; Dukor, R. K.; Nafie, L. A. *Appl. Spectrosc.* **2011**, *65*, 699.
(29) Nicu, V. P.; Mándi, A.; Kurtán, T.; Polavarapu, P. L. *Chirality* **2014**, *26*, 525.
(30) (a) Dixit, M.; Goel, A. *Tetrahedron Lett.* **2006**, *47*, 3557. (b) Goel, A.; Ram, V. J. *Tetrahedron* **2009**, *65*, 7865.
(31) (a) Goel, A.; Chaurasia, S.; Dixit, M.; Kumar, V.; Prakash, S.; Jena, B.; Verma, J. K.; Jain, M.; Anand, R. S.; Manoharan, S. S. *Org. Lett.* **2009**, *11*, 1289. (b) Goel, A.; Dixit, M.; Chaurasia, S.; Kumar, A.; Raghunandan, R.; Maulik, P. R.; Anand, R. S. *Org. Lett.* **2008**, *10*, 2553. (c) Goel, A.; Kumar, V.; Chaurasia, S.; Rawat, M.; Prasad, R.; Anand, R. S. *J. Org. Chem.* **2010**, *75*, 3656. (d) Goel, A.; Kumar, V.; Singh, S. P.; Sharma, A.; Prakash, S.; Singh, C.; Anand, R. S. *J. Mater. Chem.* **2012**, *22*, 14880.
(32) Tominaga, Y.; Ushirogouchi, A.; Matsuda, Y. J. *J. Heterocycl. Chem.* **1987**, *24*, 1557.
(33) Grimme, S. *J. Chem. Phys.* **2003**, *118*, 9095.
(34) Weigend, F.; Ahlrichs, R. *Phys. Chem. Chem. Phys.* **2005**, *7*, 3297.
(35) Sinnecker, S.; Rajendran, A.; Klamt, A.; Diedenhofen, M.; Neese, F. *J. Phys. Chem. A* **2006**, *110*, 2235.
(36) Grimme, S.; Neese, F. *J. Chem. Phys.* **2007**, *127*, 154116.
(37) Schäfer, A.; Huber, C.; Ahlrichs, R. *J. Chem. Phys.* **1994**, *100*, 5829.
(38) (a) Bringmann, G.; Bruhn, T.; Maksimenka, K.; Hemberger, Y. *Eur. J. Org. Chem.* **2009**, *2009*, 2717. (b) Bringmann, G.; Götz, D. C. G.; Bruhn, T. The Online Stereoanalysis of Chiral Compounds by HPLC-ECD Coupling in Combination with Quantum-Chemical Calculations. In *Comprehensive Chiroptical Spectroscopy*; Berova, N., Polavarapu, P. L., Nakanishi, K., Woody, R. W., Eds.; John Wiley & Sons: Hoboken, NJ, 2012; Vol. 2, p 355.
(39) (a) Bruhn, T.; Schaumlöffel, A.; Hemberger, Y.; Bringmann, G. *SpecDis*, version 1.60; University Würzburg: Würzburg, Germany, 2012. (b) Bruhn, T.; Schaumlöffel, A.; Hemberger, Y.; Bringmann, G. *Chirality* **2013**, *25*, 243.
(40) (a) Weigend, F.; Ahlrichs, R. *Phys. Chem. Chem. Phys.* **2005**, *7*, 3297. (b) Hattig, C.; Weigend, F. *J. Chem. Phys.* **2000**, *113*, 5154. (c) Christiansen, O.; Koch, H.; Jørgensen, P. *Chem. Phys. Lett.* **1995**, *243*, 409.
(41) (a) Goerigk, L.; Kruse, H.; Grimme, S. Theoretical Electronic Circular Dichroism Spectroscopy of Large Organic and Supramolecular Systems. In *Comprehensive Chiroptical Spectroscopy*; Berova, N., Polavarapu, P. L., Nakanishi, K., Woody, R. W., Eds.; John Wiley & Sons: Hoboken, NJ, 2011; Vol. 1, p 643. (b) Grimme, S.; Parac, M. *ChemPhysChem* **2003**, *4*, 292. (c) Sundholm, D. *Chem. Phys. Lett.* **2000**, *317*, 392. (d) Dreuw, A.; Head-Gordon, M. *Chem. Rev.* **2005**, *105*, 4009.
(42) Tominaga, Y. *Trends Heterocycl. Chem.* **1991**, *2*, 43.
(43) (a) Le Bahers, T.; Adamo, C.; Ciofini, I. *J. Chem. Theory Comput.* **2011**, *7*, 2498. (b) Jacquemin, D.; Le Bahers, T.; Adamo, C.; Ciofini, I. *Phys. Chem. Chem. Phys.* **2012**, *14*, 5383.
(44) The diagnosis tool DctViaCube is freely available: http://www.enscp.fr/labos/LECA/Research/site_msc/telechargement.html, accessed March 11, 2013.
(45) Frisch, M. J.; Trucks, G. W.; Schlegel, H. B.; Scuseria, G. E.; Robb, M. A.; Cheeseman, J. R.; Montgomery, J. A., Jr.; Vreven, T.; Kudin, K. N.; Burant, J. C.; Millam, J. M.; Iyengar, S. S.; Tomasi, J.; Barone, V.; Mennucci, B.; Cossi, M.; Scalmani, G.; Rega, N.; Petersson, G. A.; Nakatsuji, H.; Hada, M.; Ehara, M.; Toyota, K.; Fukuda, R.; Hasegawa, J.; Ishida, M.; Nakajima, T.; Honda, Y.; Kitao, O.; Nakai, H.; Klene, M.; Li, X.; Knox, J. E.; Hratchian, H. P.; Cross, J. B.; Bakken, V.; Adamo, C.; Jaramillo, J.; Gomperts, R.; Stratmann, R. E.; Yazyev, O.; Austin, A. J.; Cammi, R.; Pomelli, C.; Ochterski, J. W.; Ayala, P. Y.; Morokuma, K.; Voth, G. A.; Salvador, P.; Dannenberg, J. J.; Zakrzewski, V. G.; Dapprich, S.; Daniels, A. D.; Strain, M. C.; Farkas, O.; Malick, D. K.; Rabuck, A. D.; Raghavachari, K.; Foresman, J. B.; Ortiz, J. V.; Cui, Q.; Baboul, A. G.; Clifford, S.; Cioslowski, J.; Stefanov, B. B.; Liu, G.; Liashenko, A.; Piskorz, P.; Komaromi, I.; Martin, R. L.; Fox, D. J.; Keith, T.; Al-Laham, M. A.; Peng, C. Y.; Nanayakkara, A.; Challacombe, M.; Gill, P. M. W.; Johnson, B.; Chen, W.; Wong, M. W.; Gonzalez, C.; Pople, J. A. *Gaussian 09*, revision E.01; Gaussian, Inc.: Wallingford, CT, 2004.
(46) (a) Becke, A. D. *J. Chem. Phys.* **1993**, *98*, 5648. (b) Lee, C.; Yang, W.; Parr, R. G. *Phys. Rev. B: Condens. Matter Mater. Phys.* **1988**, *37*, 785.
(47) (a) Hehre, W. J.; Ditchfield, R.; Pople, J. A. *J. Chem. Phys.* **1972**, *56*, 2257. (b) Hariharan, P. C.; Pople, J. A. *Theor. Chim. Acta* **1973**, *28*, 213.
(48) Grimme, S.; Neese, F. *J. Chem. Phys.* **2007**, *127*, 154111.

DOI: 10.1021/acs.joc.6b01804
J. Org. Chem. 2016, 81, 10721–10732

(49) Schäfer, A.; Huber, C.; Ahlrichs, R. *J. Chem. Phys.* **1994**, *100*, 5829.
(50) Sinnecker, S.; Rajendran, A.; Klamt, A.; Diedenhofen, M.; Neese, F. *J. Phys. Chem. A* **2006**, *110*, 2235.
(51) (a) Neese, F. *WIREs Comput. Mol. Sci.* **2012**, *2*, 73. (b) Neese, F.; Becker, U.; Ganyushin, D.; Hansen, A.; Liakos, D.; Kollmar, C.; Koßmann, S.; Petrenko, T.; Reimann, C.; Riplinger, C.; Sivalingam, K.; Wezisla, B.; Wennmohs, F. *ORCA software package*, version 2.9.1 ed.; Max Planck Institute for Bioinorganic Chemistry: Germany, 2012.
(52) Ahlrichs, R.; Armbruster, M. K.; Bachorz, R. A.; Bär, M.; Baron, H.-P.; Bauernschmitt, R.; Bischoff, F. A.; Böcker, S.; Crawford, N.; Deglmann, P.; Della Sala, F.; Diedenhofen, M.; Ehrig, M.; Eichkorn, K.; Elliott, S.; Furche, F.; Glöß, A.; Haase, F.; Häser, M.; Hättig, C.; Hellweg, A.; Höfener, S.; Horn, H.; Huber, C.; Huniar, U.; Kattanek, M.; Klopper, W.; Köhn, A.; Kölmel, C.; Kollwitz, M.; May, K.; Nava, P.; Ochsenfeld, C.; Öhm, H.; Pabst, M.; Patzelt, H.; Rappoport, D.; Rubner, O.; Schäfer, A.; Schneider, U.; Sierka, M.; Tew, D. P.; Treutler, O.; Unterreiner, B.; von Arnim, M.; Weigend, F.; Weis, P.; Weiss, H.; Winter, N. *Turbomole*; TURBOMOLE GmbH: Karlsruhe, Germany, 2010.
(53) Weigend, F.; Ahlrichs, R. *Phys. Chem. Chem. Phys.* **2005**, *7*, 3297.
(54) Hattig, C.; Weigend, F. *J. Chem. Phys.* **2000**, *113*, 5154.
(55) (a) Bringmann, G.; Bruhn, T.; Maksimenka, K.; Hemberger, Y. *Eur. J. Org. Chem.* **2009**, *2009*, 2717. (b) Bringmann, G.; Götz, D. C. G.; Bruhn, T. In *Comprehensive Chiroptical Spectroscopy*; Berova, N., Polavarapu, P. L., Nakanishi, K., Woody, R. W., Eds.; John Wiley & Sons: Hoboken, NJ, 2012; Vol. 2, p 355.

DOI: 10.1021/acs.joc.6b01804
J. Org. Chem. 2016, 81, 10721−10732